Preprints of the 21st IFAC World Congress (Virtual)
Berlin, Germany, July 12-17, 2020

Tracking a Reference Damping Force in a Magneto-Rheological Damper for Automotive Applications

Gianluca Savaia * **Giulio Panzani** * **Matteo Corno** *
Andrea Sinigaglia ** **Sergio M. Savaresi** *

* *Dipartimento di Elettronica, Informazione e Bioingegneria, Politecnico di Milano, Milano, MI 20133, Italy.*
email: giulio.panzani@polimi.it
** *Automobili Lamborghini, Sant'Agata Bolognese, Italy*

Abstract: Magneto-rheological dampers are gaining a lot of attention in the automotive industry and they show many advantages over their hydraulic counterpart. However, they are characterised by a highly nonlinear damping characteristics which may not be desired. In this paper, the authors present a control scheme which gives the possibility to track any reference damping force in a magneto-rheological damper. The main assumption of this research is the actual force exerted by the damper is not available for measurement, since such a sensor could not be installed onto a commercial vehicle. The control of this device is particularly challenging because of a singularity point in the origin which has significant repercussions on performance if not considered. The authors propose a novel closed-loop technique which is compared against an industrial solution based on an open-loop scheme, proving the former to be superior via a qualitative and quantitative analysis.

Keywords: Magnetic Suspension, Semi-Active Dampers, Tracking characteristics, Feedback Control Methods, Open-loop control systems

1. INTRODUCTION

Magneto-rheological fluid can change its viscosity when subjected to a magnetic field, Olabi and Grunwald (2007): such property has been successfully exploited to design semi-active dampers in which the current flowing into a solenoid induce the change of fluid viscosity and thus the resulting damping force. The application of magneto-rheological (MR) dampers for the purpose of vibration control has been widely investigated in the past years. These devices gained particular interest also within the automotive community, after being successfully deployed into the suspension system of sports-cars as Ferrari 599GTB, Audi TT and Lamborghini Aventador; in these extreme vehicles, such dampers play a significant role in the control of the vertical dynamics since they can exert high forces even at very low stroke speed.

There exists an extensive literature dealing with the control of the vertical vehicle dynamics Savaresi et al. (2005); Savaresi and Spelta (2007); however such control strategies (*e.g.*, skyhook) are typically designed assuming a linear damping behaviour of the suspension. MR dampers, on the opposite, show a highly nonlinear characteristics and for this reason a low-level control strategy is usually introduced in the control architecture, aiming at smoothing the device nonlinearities eventually reshaping its behaviour so to mimic a linear one, see *e.g.* Corno et al. (2019).

Dealing with the damper nonlinear behaviour is a known issue and previous work on the subject can be found in the scientific literature: in Sims et al. (1997, 1999, 2000); Sims (2006) the authors started investigating the control problem for electro-rheological devices which, differently from magneto-rheological damper, make use of an electric field to control vibrations. They propose a simple closed-loop system aimed at linearising the Bingham-type constitutive relationship of such devices; further work Batterbee and Sims (2005) started investigating the applications in the automotive industry, and in Batterbee and Sims (2007, 2009) the authors set up a hardware-in-the-loop simulation, where the actual damping force was measured from a test rig. Similarly, in Weber (2015) and Ho et al. (2013), the control problem is applied to an experimental setup where the force is assumed to be measurable and therefore a feedback scheme is employed.

An open-loop approach have been investigated by different authors in Seong et al. (2009); Weber (2013), where they exploit the inverse Bingham model to impose a desired reference force, and in Lee and Choi (2000) which exploits a fluid-dynamics model to derive the current signal to be applied to the magneto-rheological damper. A similar open-loop strategy is experimentally employed in an earlier work of the authors Corno et al. (2019), where attention is also paid to the undesired fluctuations of the control variable (*i.e.* the current flowing in the solenoid) naturally arising from the open-loop approach.

In the present work a closed-loop strategy is proposed, that allows the tracking of a desired damping characteristics, for a MR damper used in automotive applications. Since the damping force is not directly measurable, the closed-

loop strategy is based on a control-oriented model of the damper which acts as a *virtual sensor*. The proposed approach is compared to a naiver open-loop scheme; it is shown how the closed-loop outperforms the open-loop strategy considering both the force tracking performance and the control variable fluctuations.

The remainder of this paper is as follows. In Section 2, the working principle and modelling of a magneto-rheological damper are presented. In Section 3, the reference tracking problem is discussed and two possible methodologies to tackle the control problem are proposed; their comparison is traced in Section 4. The paper ends with some concluding remarks and future activities aimed at validating experimentally the proposed work. Throughout the paper, for confidentiality reasons, the axes of some Figures have been concealed.

2. MR DAMPER MODELLING

A damper typically consists of the oil chamber, the piston and a gas chamber. As the piston moves, pushed or pulled by external forces (e.g., the movement of the wheel), the fluid is forced through the orifices of the piston head which build up resistance against the fluid flow; this friction force is proportional to the speed of the movement and the relation between these two quantities (force and speed) goes by the name of damping characteristics. In a magneto-rheological damper (MR damper), the consistency of the fluid can be changed in real-time, thanks to smart fluids which can rapidly modify their characteristics when subjected to a magnetic field, Olabi and Grunwald (2007). It is then possible to control the damping characteristics via the applied current at high frequencies.

Generically, a MR damper is modelled as a relationship

$$F_{MR} = f(I, \dot{z}),$$

where F_{MR} is the friction force (output) depending on the applied current I (control input) and rod speed movement $\dot{z}$ (exogenous input). In literature, many have attempted to describe this nonlinear relationship and a thorough review may be found in Wang and Liao (2011).

In this work, we consider a control-oriented model for the MR damper

$$\begin{cases} \dot{I} = -\alpha I + \alpha I_{ref} \\ F_{MR} = f(I, \dot{z}) \end{cases}, \tag{1}$$

where the nonlinear static equation of the force-speed damping characteristics is flanked by a linear differential equation modelling the current actuation dynamics. Instead of using a more common physically-inspired approach to model the nonlinear damping characteristics, a data-driven non-parametric point of view has been preferred.

The static relationship f in equation (1) has been characterised via sinusoidal excitation experiments performed at the test bench; the resulting force-speed curves are shown in Figure 1 for different constant currents, where a monotonic relation holds for the damping force with respect to the stroke speed and the applied current. Accordingly, f describes the linear interpolation of these curves.

The actuation dynamics in (1) is a low-pass filter whose cutoff frequency has been identified experimentally in order to minimise the prediction error between the measured force recorded by the test bench and the MR damper model.

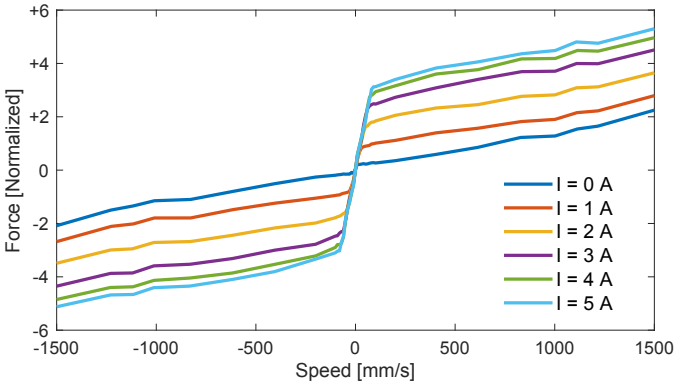

Fig. 1. Experimental static damping characteristics of a MR damper.

The experimental validation of the proposed model (1) is shown in Figure 2, where the damper was solicited with a real stroke profile and a pseudo-random control current.

To conclude the modelling of the MR damper, it is worth noticing that, consistently with the strictly passive domain of the device, every damping curve pass through the origin:

$$\forall I,\ F_{MR} = f(I, 0) = 0.$$

This implies that the system is neither controllable nor reachable when there is no stroke movement: no matter the amount of current injected into the piston's head, the damper's output force is zero. This is a relevant property that will affect the control performances in a neighbourhood of this singularity point.

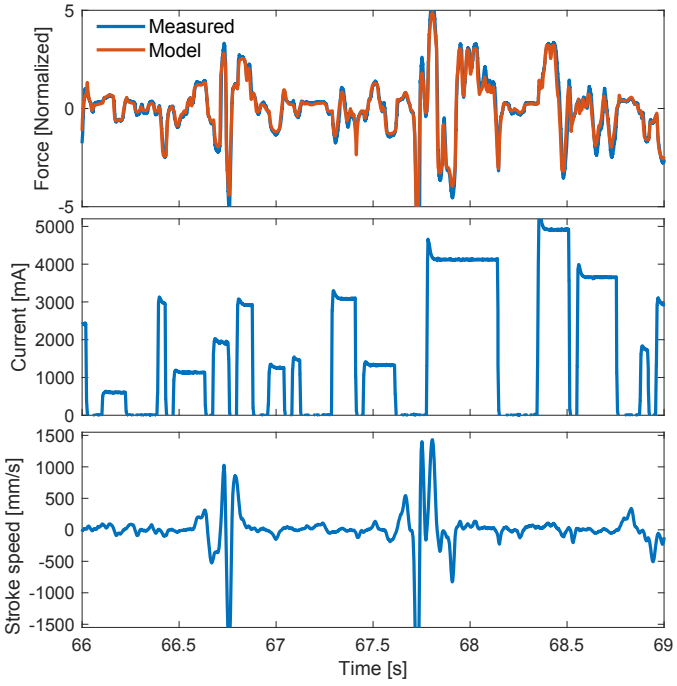

Fig. 2. Validation of the proposed control-oriented model force results (top) for a realistic road profile (bottom) with varying input current (middle).

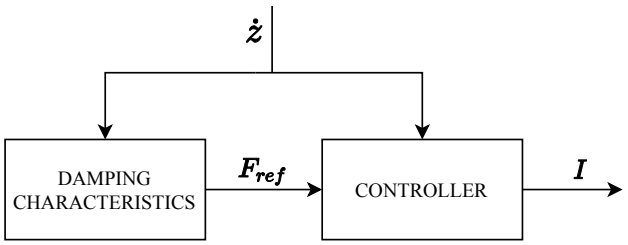

Fig. 3. Force tracking control scheme.

3. DAMPING FORCE REFERENCE TRACKING

The main objective of the proposed control schemes is to define a strategy with which any desired damping characteristics can be tracked, namely overriding the constant current damping curves of the MR damper. This is motivated by the need of giving a different shape to the damping characteristics which, as visible in the experimental curves shown in Figure 4, is very steep for low stroke speeds, causing discomfort to the passengers of the vehicle.

To achieve the aforementioned objective, a force tracking control scheme must be developed, whose architecture is shown in Figure 3. The block denominated *Damping characteristics* contains the shape of the desired damping curve, expressed as function of the stroke speed $\dot{z}$; it is important that any designed curve lies within the controllability region of the suspension, namely the area in the force-speed diagram comprised within the minimum and maximum damping characteristics (the $0A$ and $5A$ curves in Figure 1).

Finding the optimal shape of the damping curve is very application dependent and it is out of the scope of this research; in this work, two classes of functions are considered:

$$F_{ref} = C\dot{z}, \qquad C > 0$$
$$F_{ref} = \alpha \tanh \beta \dot{z}, \qquad \alpha > 0, \beta > 0$$

The first expression *linearises* the MR damper characteristics with respect to the stroke speed, allowing to emulate an ideal linear damper; the second expression defines a more complex – nonlinear but smooth – curve, where the parameter α and β allow one to shape the slope and amplitude of the damping effect. A qualitative example for both curves is provided in Figure 4.

The output of the *Damping characteristics* block is a reference force F_{ref} which is fed to the actual *Controller* which is in charge of modulating the current I needed to deliver such damping force by the MR damper. In the following, two possible solutions for this block are discussed: the open-loop implementation and the proposed closed-loop scheme.

3.1 Open-loop Control

One option to control a MR damper (see *e.g.* Seong et al. (2009); Weber (2013); Corno et al. (2019)) is by means of the inverse model of the static term of equation (1)

$$I_{OL} = f^{-1}(F_{ref}, \dot{z}). \tag{2}$$

This solution is commonly implemented by means of look-up tables, mapping the inverse model as shown in Figure 5. At any given time, the stroke speed $\dot{z}$ is read, and the corresponding reference force F_{ref} is provided by the *Damping characteristics* block: these two quantities are then fed to the controller which returns the exact amount of current to track the desired damping force. The inverse map approach neglects the dynamic term of the MR model (1), typically assuming the actuation dynamics to have a much wider bandwidth than the system we aim to control. For this reason, even when the inverse damper model is perfectly known, an inaccurate dynamic tracking of the reference force must be expected.

The main advantage of this scheme is that it is possible to derive a unique relationship between rod speed $\dot{z}$ and output current I

$$I_{OL} = f^{-1}(F_{ref}(\dot{z}), \dot{z}) = f^{-1}(\dot{z})$$

since the reference force F_{ref} expressed as sole function of the stroke speed, as previously discussed. This bijective relationship yields repeatable performance since for any speed and reference force, there exists a unique value of current. Further, this controller has no tuning parameter: once the the static model of the MR damper is provided, the inverse function f^{-1} is straightforward.

On the other hand, the main issue of this implementation lies in the singularity point present in the origin: at zero

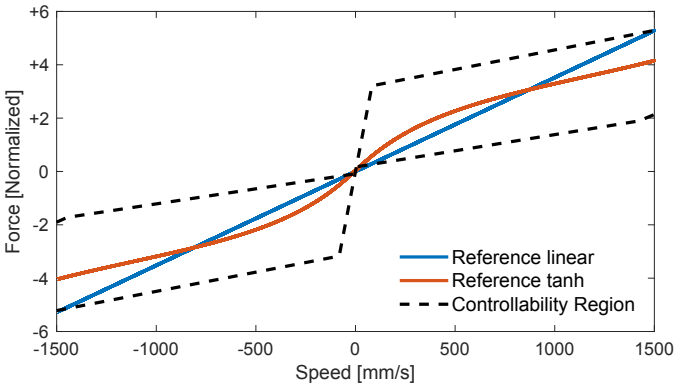

Fig. 4. Examples of possible damping characteristics which can be emulated. The dashed line represents the physical limits of the MR damper.

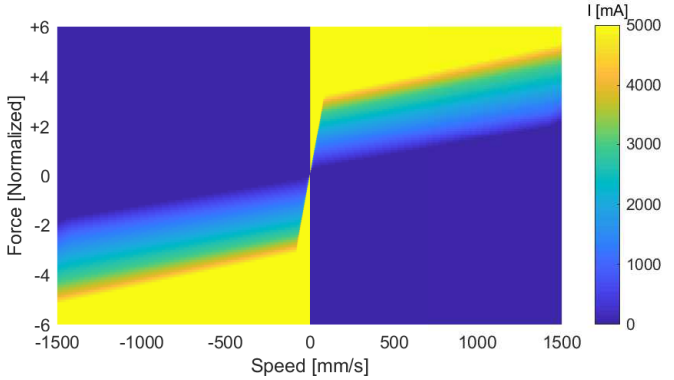

Fig. 5. The look-up table implementing the inverse model (2) used in the open-loop controller; outside the controllability region, the current is saturated between its minimum and maximum.

stroke speed, any current yields zero force. A common solution that retains the bijective relationship is to assign an arbitrarily constant current value to the singularity point, typically setting it to zero for the sake of reducing the device energy consumption.

$$I_{OL} = f^{-1}(0) = 0.$$

With the proposed choice, every time the rod changes direction of movement (*i.e.*, every time there is a zero crossing of the stroke speed), the output current I jumps to zero regardless the value assumed before the zero crossing. As a matter of fact, any small perturbation of $\dot{z}$ in the low speed region of the damper characteristics may result in fast and notable jumps of the current.

As it will be shown in Section 4, the control signal visibly *chatters* while attempting to track the reference force for low speeds. Although, from a mathematical point of view, this should not make any difference ($F_{MR} = f(I, 0) = 0, \quad \forall I$), from a practical point of view it has been observed the filtering performance of the damper suffer from these big jumps. Such undesired behaviour could be practically patched by means of nonlinear elements (*e.g.*, deadzones), but these would introduce a whole other set of issues to the detriment of the control problem.

3.2 Closed Loop Control

The closed-loop framework proposed in this paper tackles the control problem from a different perspective: whereas in Section 3.1 the controller exploited the inverse model to output a current, here the model is employed as a *virtual sensor*, to estimate the present damping force (the actual damping force cannot be directly measured) and feedback this information to ultimately adjust the control current. As discussed in the following, such approach naturally avoids the detrimental chattering effect of the singularity point in the origin. It should also be noticed that the closed-loop controller is not more robust against uncertainties with respect to the open-loop framework, since they both rely on the same model: the former exploits the direct model equations, whilst the latter the inverse one.

The MR damper model observer estimates the present damping force F_{est} from the current I and rod speed $\dot{z}$. This estimation is used to generate an error signal $e = F_{ref} - F_{est}$, whose sign depends on the present state of the rod. During compression the forces are positive by convention (see Figure 1): if $F_{ref} > F_{est}$ then the error is positive and the current is correctly increased until it matches the reference. During extension the forces are negative by convention: if $-|F_{ref}| > -|F_{est}|$ then the error is negative and the current is mistakenly decreased. This is the reason why the error shall change sign according to the present rod speed.

The controller $R(s)$ employed is in the form of a simple integral controller:

$$R(s) = \frac{K}{s},$$

where K is the integral control gain; the architecture of the control scheme is depicted in Figure 6, and the output control current is therefore

$$I_{CL} = R(s)(F_{ref} - F_{est})sign(\dot{z}) \tag{3}$$

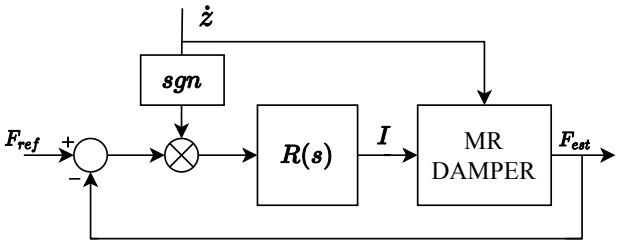

Fig. 6. Schematic representation of the closed-loop controller: the model observer estimates the damping force, and a control law $R(s)$ computes the current I sent out to the actual device.

where F_{est} is described by equation (1) and F_{ref} is the output of the *Damping characteristics* block in Figure 3.

The main advantage of this formulation is that the arbitrary inversion of the singularity point required in the open loop approach is no longer an issue in the closed-loop one. In fact, when the rod changes direction (*i.e.*, approaching a zero-crossing) the integrator naturally holds the past value of the current, thus avoiding to *chatter* because of the singularity. Indeed, for $\dot{z} = 0$, we have that $F_{ref} = F_{est} = 0 \implies e = 0$, and thus the integrator state is not updated. It should be noticed that the nice bijective property which characterised the open-loop solution is lost, since now the control law is described by the differential equation (3) rather than the algebraic one in (2).

The calibration parameter of the closed-loop approach is the controller gain K, which is expected to affect the tracking performance: low values of K would yield a low bandwidth tracking dynamics, not suitable to match the fast changing force references. Opposite, a higher value could compromise the closed-loop system stability, again leading to a poor tracking of the reference force.

4. VALIDATION AND COMPARISON

In this section, the two control strategies are compared against each other in simulation.

4.1 Qualitative Analysis

The two control strategies are compared against when a rod excitation follows a real measurement from an actual vehicle on a country road: the result of the proposed simulation is represented in Figure 7. Although the force tracking performance is similar for both schemes, the current *chattering* issue is visibly remarked for the open-loop controller. From Figure 7, it is clear that this phenomenon is not isolated to occasional events but it is occurring throughout the experiment. As mentioned, the origin of this issue is better appreciated by zooming-in a detail of a zero crossing, as shown in Figure 8, where it is possible to see the current spikes in the open-loop controller, whilst the closed-loop framework has a much more elegant behaviour.

It is also important to remark how the current spikes of the open-loop scheme do not have any visible effect

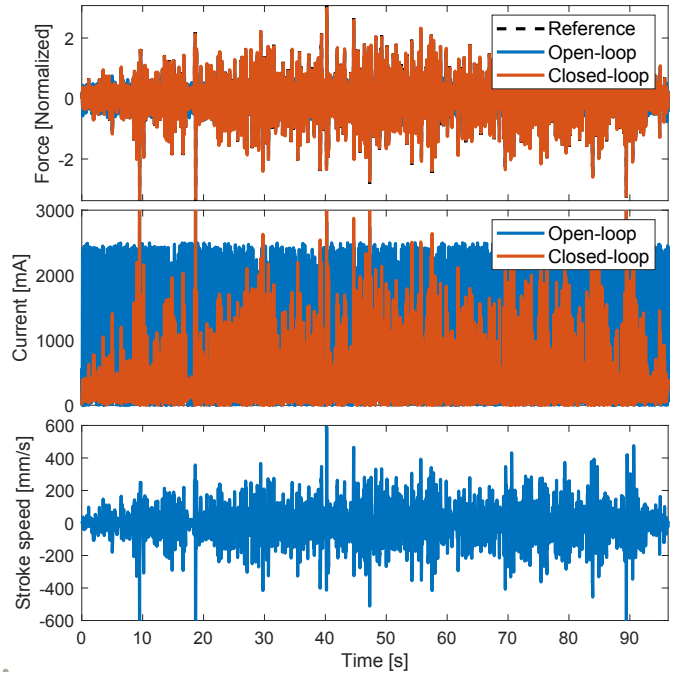

Fig. 7. Overall simulation comparison of the two strategies using a realistic road profile.

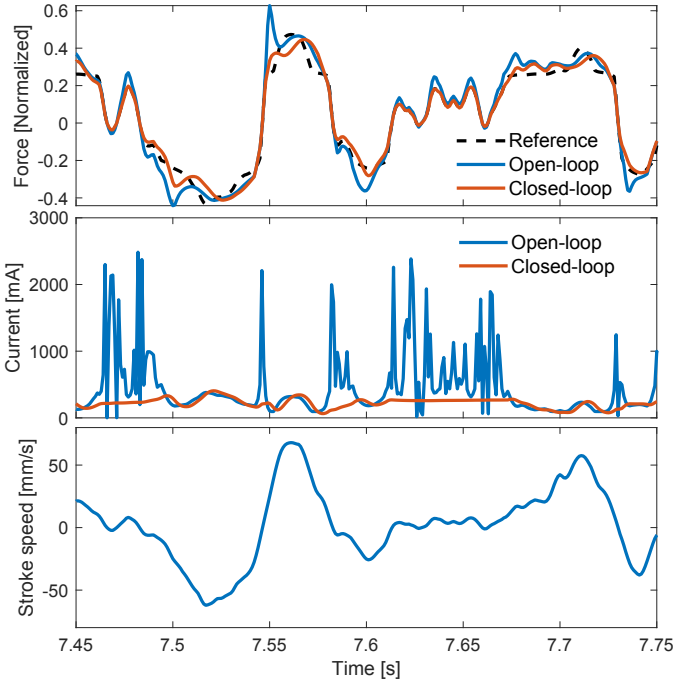

Fig. 8. Detail of the *chattering* phenomenon when stroke speed is in a neighbourhood of zero.

on the force estimated by the mathematical model in equation (1) but, in practice, they have a detrimental impact on performance as discussed in Corno et al. (2019). Indeed, the effectiveness of the tracking capabilities of both approaches is shown in Figure 9 where the rod is excited by a sinusoidal displacement which sweeps the whole speed range of interest. Both reference curves (linear and hyperbolic tangent) can be tracked by the proposed controllers, other than the hysteretic behaviour which is due to the actuation dynamics.

4.2 Quantitative Analysis

In order to provide a quantitative comparison of the two approaches, two performance indexes are proposed:

$$J_{tracking} = \sqrt{\frac{1}{T}\int_0^T (F_{ref} - F_{est})^2\, dt} \tag{4}$$

$$J_{control} = \sqrt{\frac{1}{T}\int_0^T \left(\frac{dI}{dt}\right)^2 dt} \tag{5}$$

where F_{ref} is the reference force, F_{est} the one estimated by the model in (1), I is the control current and T the experiment time duration. Hence, $J_{tracking}$ weighs the tracking performance and $J_{control}$ the control action.

As discussed in Section 3, the open-loop strategy does not consider any parameter, whereas in the closed-loop scheme the integral gain K must be calibrated. In Figure 10, the performance of the two schemes are compared against each other for the realistic road test and, for the closed-loop, the sensitivity to K is displayed to draw a pareto curve. The values of the performance indexes are normalised with respect to the worst case.

As expected, a trade-off in the choice of K arises, when the focus is set only on the tracking performances. Opposite, the chattering index has a monotonic trend: intuitively,

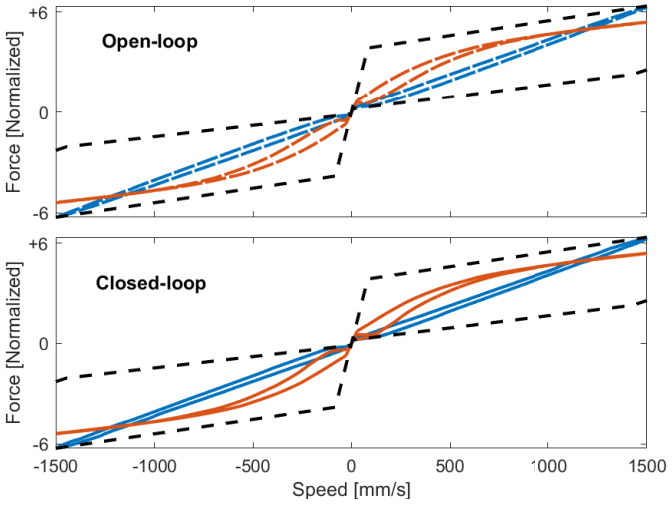

Fig. 9. Resulting force when emulating the reference curve in Figure 4 for the open-loop and closed-loop strategies.

the higher the controller gain, the higher the closed-loop bandwidth and thus the required control action to match the high frequency varying reference. As shown in Figure 10, there exists a set of control gains K for which the closed-loop strategy shows better performance, both in tracking and control, with respect to the open-loop approach, thus proving the advantages of the closed-loop scheme.

5. CONCLUSIONS

In this paper, a comparison between two control strategies for the tracking of the damping force in a MR damper have been presented: an open-loop scheme, which is easier to implement and makes use of the inverse model of

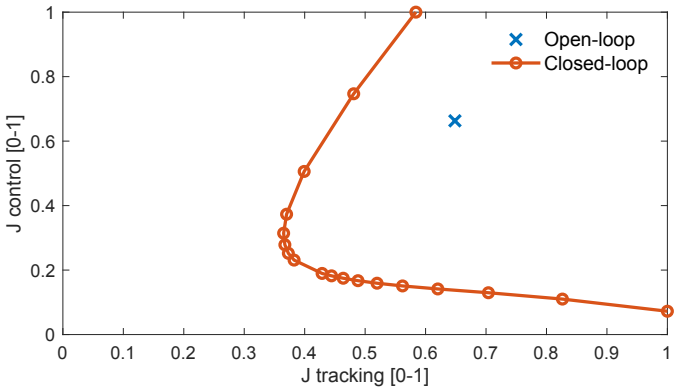

Fig. 10. Performance indexes of the control strategies. The sensitivity to the control gain K (increasing from the bottom right) is shown for the closed-loop scheme.

the damping characteristics, and a closed-loop one which employs directly the MR damper model as a virtual sensor and compute the control current to reduce the force tracking error.

Both controllers allow to shape any desired damping characteristics, overriding the (undesired) natural curves of the MR damper; such feature has been proved to be essential by studies on vehicle vertical dynamics control with MR dampers.

It has been shown that the open-loop scheme misbehaves in a neighbourhood of the origin of the force-speed phase diagram. In particular, when the rod movement changes direction, this controller generates current spikes which do not improve the tracking performance and are detrimental to the driving comfort. The closed-loop controller has been introduced to cope with this issue, and it has been shown to be a much more flexible framework to deal with this problem, leading to better force tracking along with a significant reduction of the control variable chattering.

The results summarised in this manuscript rely on the accuracy of the damper model, since it is not possible to measure the actual damping force on the vehicle in real-time. As a further validation of the proposed work, this algorithm shall be validated on a test bench equipped with a load cell.

ACKNOWLEDGMENTS

The authors thank Automobili Lamborghini for providing the magneto-rheological damper, without which this research would have not been possible.

REFERENCES

Batterbee, D. and Sims, N.D. (2009). Temperature sensitive controller performance of mr dampers. *Journal of Intelligent Material Systems and Structures*, 20(3), 297–309.

Batterbee, D. and Sims, N. (2005). Vibration isolation with smart fluid dampers: a benchmarking study. *Smart Structures and Systems*, 1(3), 235–256.

Batterbee, D. and Sims, N. (2007). Hardware-in-the-loop simulation of magnetorheological dampers for vehicle suspension systems. *Proceedings of the Institution of Mechanical Engineers, Part I: Journal of Systems and Control Engineering*, 221(2), 265–278.

Corno, M., Galluppi, O., Panzani, G., Sinigaglia, A., Capuano, P., Cecconi, J., and Savaresi, S.M. (2019). Design and validation of a full body control semi-active suspension strategy for a supercar. *IFAC International Symposium on Advances in Automotive Control*.

Ho, C., Lang, Z., Sapiński, B., and Billings, S. (2013). Vibration isolation using nonlinear damping implemented by a feedback-controlled mr damper. *Smart Materials and Structures*, 22(10), 105010.

Lee, H.S. and Choi, S.B. (2000). Control and response characteristics of a magneto-rheological fluid damper for passenger vehicles. *Journal of Intelligent Material Systems and Structures*, 11(1), 80–87.

Olabi, A.G. and Grunwald, A. (2007). Design and application of magneto-rheological fluid. *Materials & design*, 28(10), 2658–2664.

Savaresi, S.M., Silani, E., and Bittanti, S. (2005). Acceleration-driven-damper (add): An optimal control algorithm for comfort-oriented semiactive suspensions. *Journal of dynamic systems, measurement, and control*, 127(2), 218–229.

Savaresi, S.M. and Spelta, C. (2007). Mixed sky-hook and add: Approaching the filtering limits of a semi-active suspension. *Journal of dynamic systems, measurement, and control*, 129(4), 382–392.

Seong, M.S., Choi, S.B., and Han, Y.M. (2009). Damping force control of a vehicle mr damper using a preisach hysteretic compensator. *Smart materials and structures*, 18(7), 074008.

Sims, N., Stanway, R., and Beck, S. (1997). Proportional feedback control of an electro-rheological vibration damper. *Journal of intelligent material systems and structures*, 8(5), 426–433.

Sims, N., Stanway, R., Peel, D., Bullough, W., and Johnson, A. (1999). Controllable viscous damping: an experimental study of an electrorheological long-stroke damper under proportional feedback control. *Smart materials and structures*, 8(5), 601.

Sims, N.D. (2006). Limit cycle behavior of smart fluid dampers under closed loop control. *Journal of vibration and acoustics*, 128(4), 413–428.

Sims, N.D., Stanway, R., Johnson, A.R., Peel, D.J., and Bullough, W.A. (2000). Smart fluid damping: shaping the force/velocity response through feedback control. *Journal of intelligent material systems and structures*, 11(12), 945–958.

Wang, D. and Liao, W.H. (2011). Magnetorheological fluid dampers: a review of parametric modelling. *Smart materials and structures*, 20(2), 023001.

Weber, F. (2013). Bouc–wen model-based real-time force tracking scheme for mr dampers. *Smart Materials and Structures*, 22(4), 045012.

Weber, F. (2015). Robust force tracking control scheme for mr dampers. *Structural Control and Health Monitoring*, 22(12), 1373–1395.